Journal of
Nanoscience and Nanotechnology
Vol. 6, 990–995, 2006

Synthesis of "Cactus" Top-Decorated Aligned Carbon Nanotubes and Their Third-Order Nonlinear Optical Properties

P. H. Li,[1] Y. L. Qu,[1] X. J. Xu,[1] Y. W. Zhu,[1] T. Yu,[1] K. C. Chin,[1,4] J. Mi,[1] X. Y. Gao,[1] C. T. Lim,[2] Z. X. Shen,[3] A. T. S. Wee,[1,4] W. Ji,[1,*] and C. H. Sow[1,4,*]

[1] *Department of Physics, BLK S12, Faculty of Science, National University of Singapore, 2 Science Drive 3, Singapore, 117542*
[2] *Department of Mechanical Engineering & Division of Bioengineering, National University of Singapore, Singapore, 117576*
[3] *School of Physical & Mathematical Sciences, Nanyang Technological University 1 Nanyang Walk, 637616, Singapore*
[4] *National University of Singapore Nanoscience and Nanotechnology Initiative, Singapore*

We report a new morphology of "cactus" top-decorated aligned carbon nanotubes grown by the PECVD method using pure C_2H_2 gas. Unlike most previous reports, no additional carrier gas is used for pretreatment. Carbon nanotubes can still grow and maintain the tubular structure underneath the "cactus" tops. It is proposed that the H atoms produced by the dissociation of C_2H_2 activate the catalyst nanoparticles. Scanning electron microscopy (SEM) shows that the top "cactus" morphology is composed of a large quantity of small nanosheets. Transmission electron microscopy (TEM) reveals the amorphous carbon nature of these "cactus" structures. The formation of these "cactus" structures is possibly due to covalent absorption and reconstruction of carbon atoms on the broken graphite layers of nanotubes produced by the strong ion bombardment under plasma. The third-order optical nonlinearities and nonlinear dynamics are also investigated. The third-order nonlinear susceptibility magnitude $|\chi^{(3)}|$ is found to be $2.2 \times 10^{-11} esu$, and the relaxation process takes place in about 1.8 ps.

Keywords: Carbon Nanotubes, Catalyst, Nonlinear Optical Properties.

1. INTRODUCTION

Since their discovery in 1991, carbon nanotubes (CNTs) have attracted great interest due to their outstanding structural, electrical and mechanical properties.[1–3] CNTs with different morphologies,[4–6] have been reported by using different synthesis methods. Among them, plasma-enhanced chemical vapor deposition (PECVD),[7,8] is a commonly used technique for the synthesis of aligned carbon nanotube array films on a substrate that is coated with a catalyst metal thin film. The growth process involves the dissociation of hydrocarbon molecules on the metal nanoparticle surface, the dissolution and saturation of carbon atoms in the catalytic particles, and the precipitation from the particles.[2] Generally, the metal film is pretreated by ammonia or hydrogen gas in order to form catalytic particles in nanometer size, which produce effective catalysts for the nanotube growth. The size of these particles is related to the diameter of CNTs. A previous study showed that carbon nanotubes could not be grown, using a recipe whereby C_2H_2 was introduced first, followed by NH_3 via plasma enhanced hot filament chemical vapor deposition (PE-HF-CVD) method.[7] Amorphous carbon produced in the C_2H_2 plasma coated on the catalyst surface and inhibited the catalytic role of catalyst particles.[7] Recently, it was found that multi-walled carbon nanotubes (MWNTs) can be grown with pure C_2H_2 by thermal CVD method with H_2/N_2 mixed gas pretreatment.[9] However, the density of the as-grown MWNTs is low, and the length is shorter compared with those grown with C_2H_2/H_2, C_2H_2/Ar, or C_2H_2/N_2 mixture gas.

Here we report "cactus" top-decorated aligned carbon nanotubes grown without NH_3 or H_2 gas pretreatment by the PECVD method. It is found that C_2H_2 gas not only acts as a carbon source but also activates the catalysts for nanotube growth under the plasma. The "cactus" morphology appears only on the top part of nanotubes while the lower body of the nanotubes retains the multi-walled structure. The third-order optical nonlinearities and nonlinear dynamics were also investigated. The large surface area of the "cactus" morphology is expected to improve the

*Authors to whom correspondence should be addressed.

 1533-4880/2006/6/990/006 doi:10.1166/jnn.2006.167

absorption capacity of gas or biological molecules, making it potentially useful for gas and biosensor applications.

2. EXPERIMENTAL DETAILS

In this work, "cactus" nanotubes were grown in a rf (13.56 MHz) plasma-enhanced chemical vapor deposition (PECVD) system. An iron film with a thickness in the range 5–100 nm was deposited on the silicon/quartz substrate by rf magnetron sputtering. The iron coated substrates were heated up to 700 °C gradually at a base pressure of 10^{-6} Torr. After that, C_2H_2 gas (15 sccm) was then introduced into the PECVD system. The working pressure and rf power were maintained at 60 mTorr and 100 W, respectively. In the same PECVD system, normal multi-walled carbon nanotubes are grown by using the same PECVD under a mixed reactant gas flow (C_2H_2/NH_3, 15 sccm/30 sccm) at around 700 °C for 1 h. Scanning electron microscopy (SEM JEOL JSM-6400F), high-resolution transmission electron microscopy (HRTEM, JEOL JEM-2010F operated at 200 kV), and Micro-Raman spectroscopy (Jobin Yvon T64000 system; Ar ion laser with wavelength of 514.5 nm) were used to study the formation of "cactus" decorated aligned nanotubes. X-ray photoelectron spectroscopy (XPS) measurements were performed at the soft X-ray beamline at the Singapore Synchrotron Light Source (SSLS).[10] The energy of the incident X-rays used is 700 eV. To evaluate the third order nonlinearities as well as the relaxation dynamics of these MWCNTs on quartz, open aperture and close aperture Z scan as well as the degenerate pump probe experiments were performed at 780 nm. The laser pulses have 220 fs full width at half maximum (FWHM) temporal pulse width and 1 kHz repetition rate generated by a Ti: sapphire regenerate amplifier (Quantronix, Tian) which is seeded by a mode locked Ti: sapphire regenerate laser (Quantronix, IMRA).

3. RESULTS AND DISCUSSION

SEM images of "cactus" nanotubes grown for 1 h are shown in Figure 1. "Cactus" knob morphology is observed from the top view image in Figure 1(a). The side-view image in Figure 1(b) shows that the "cactus" morphology appears only at the top, while the lower part of the nanotubes retain the aligned structure. The length of nanotubes is about 10 μm. The side-view image in Figure 1(c) shows that the "cactus" structures are bundled together. Figure 1(d) reveals the "cactus" morphology is composed of a large quantity of small nano-sheets with thickness about 1–2 nm. The diameter of the "cactus" part is about 300 nm, while the diameter of the as-grown normal MWNT is about 20–40 nm.

Figure 2 shows the Raman spectra of "cactus" top-decorated nanotubes and multi-walled nanotubes. In this case, the normal multi-walled carbon nanotube sample was

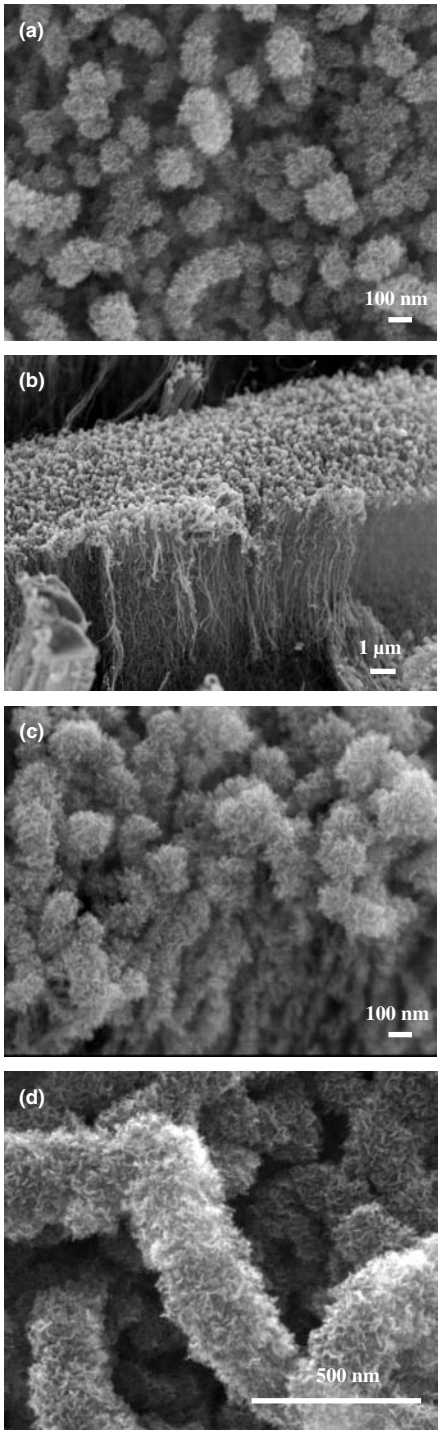

Fig. 1. (a) SEM image of "cactus" carbon nanotubes from the top view. (b) Side-view picture shows that the cactus structure on the top part of nanotube while the underneath part still remain the aligned structure. (c) Close-up view of the "cactus" structure on the top part. (d) HRSEM picture of "cactus" nanotubes shows the rough "cactus" surfaces is composed of a large quantity of nano-sheets.

grown on a Si substrate using PECVD under a reactant gas flow (C_2H_2/NH_3, 15 sccm/30 sccm) at around 700 °C for 1 h. Previous studies show that for multi-walled CNTs, the G-band corresponds to graphite or ordered carbon, while

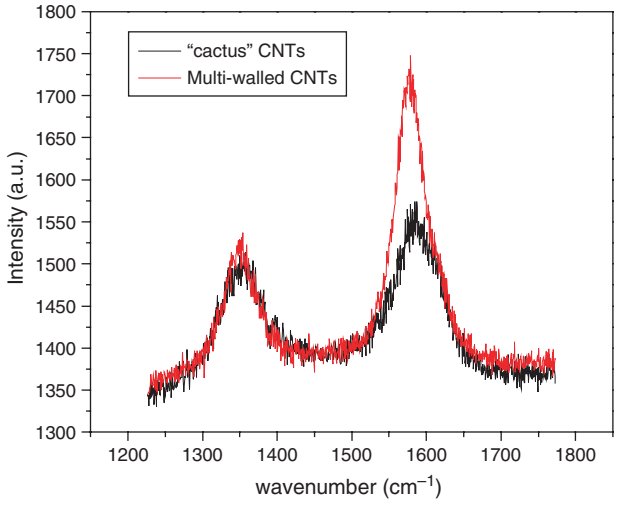

Fig. 2. Raman spectra for "cactus" nanotube and MWNT grown for 1 h.

the D-band indicates disordered or amorphous carbon.[11] In addition, the line width of D-band is related to the amount of amorphous carbon.[12] Based on the curve fitting results, we obtained the ratio (I_D/I_G) of "cactus" nanotube is about 0.75 ± 0.10, while the ratio is only 0.43 ± 0.05 for normal multi-walled CNT. In addition, a larger line width of D-band is obtained for "cactus" nanotube. This Raman study indicates a higher amorphous carbon content in "cactus" nanotubes compared with C_2H_2/NH_3 grown multi-walled CNT.

Figure 3(a) shows a typical TEM image of the "cactus" nanotubes lying on the carbon film of a TEM Cu grid. Close-up views at three regions in Figure 3(a) are shown in Figure 3(b) to (d). Figure 3(b) shows the amorphous structure of the top "cactus" part: the layers are not regular and do not have specific orientations. Figure 3(c) shows the intermediate part between the top amorphous carbon and the nanotube. It can be seen that some of the graphite layers are broken, and this could be attributed to the strong ion bombardment under plasma during the growth process. These broken layers provide a rich source of dangling bonds for the covalent absorption of activated carbon atoms from the dissociated C_2H_2 precursor. Figure 3(d) clearly shows that some outer graphite layers of a nanotube are peeled off and only thinner inner layers are left. The electron diffraction pattern further reveals the disordered graphite structure of these "cactus" top-decorated nanotubes. The calculated spacing between different layers of nanotubes is 3.41 Å, matching the layer spacing in graphite. The XRD pattern (not shown) is similar to that of graphite, but the main peak (002) is much weaker and broadened.

XPS study was carried out to investigate the surface chemical states on the surface of "cactus" and normal multi-walled carbon nanotubes. The contributions of photoelectrons from the diamond-like SP^3 component and graphite SP^2 component can be separated by peak fitting the XPS spectra as shown in Figure 4. The C 1s spectra

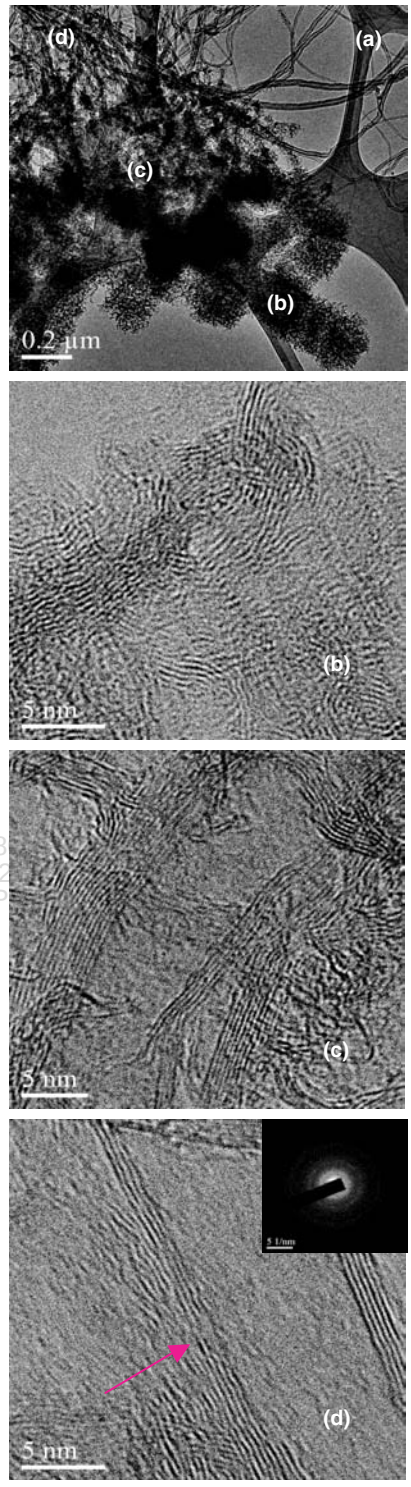

Fig. 3. (a) Typical HRTEM picture of "cactus" top-decorated nanotube bundles. (b) Amorphous carbon on the top part with no encapsulated catalytic particles. (c) The intermediate part between the amorphous carbon and the lower nanotube body. It shows that the nanotube surface is destroyed and linked with some amorphous carbon. (d) For the lower body of the nanotube, it can be seen that some graphite layers are broken (marked by the arrow), but the absorption of C atoms become less compared with part (c). ED pattern (Inset) reveals the disordered graphite structure of "cactus" nanotube, the calculated spacing between different layers is 3.41 Å, matching the layer spacing in graphite.

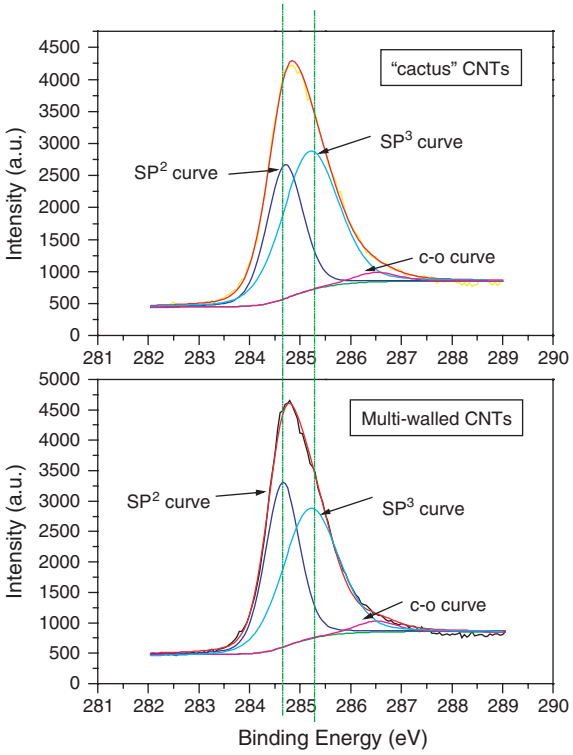

Fig. 4. XPS spectra of C 1s peak for Multi-walled and "cactus" CNTs. Both samples were fitted with component peaks at 284.7, 285.2, and 286.5, which correspond to SP^2, SP^3, and C=O or C−O bond.

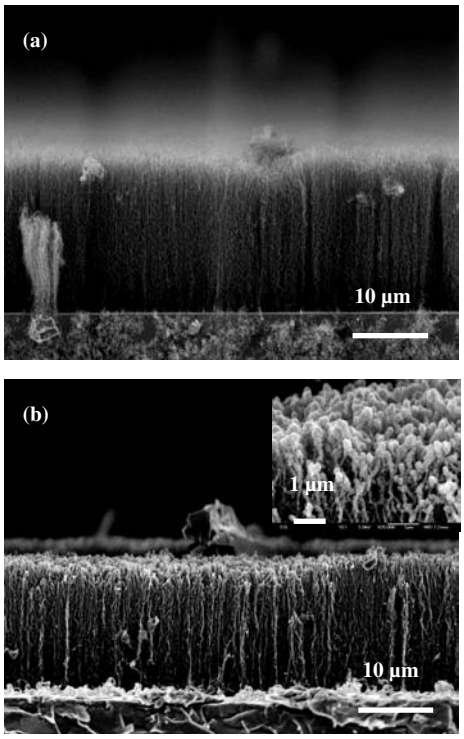

Fig. 5. (a) is the SEM picture for the as-grown MWNT sample 1(C_2H_2/NH_3, 20 mins), the length of the nanotube is about 20 μm. (b) Re-grown MWNT under C_2H_2 plasma for 1 h followed the growth procedure of "cactus" nanotube. "Cactus" morphology is observed on the top part, while the length of re-grown nanotube is slightly shorter than the as-grown one.

of both samples were fitted with the component peaks at 284.7, 285.2, and 286.5 eV, which correspond to SP^2, SP^3, and C=O or C−O bonds respectively.[13, 14] The SP^3/SP^2 ratios (calculated from the ratio of the areas of the SP^3 and SP^2 peak[15]) for the "cactus" nanotube and MWNTs are 1.59 ± 0.06 and 1.13 ± 0.04 respectively. Although a higher SP^3 component is obtained for "cactus" nanotubes, no crystalline diamond particle has been observed. Generally, SP^3C could be bonded to either C or H. A previous study has shown that the hydrogen termination plays an important role in diamond crystallization and growth.[16] In this case, most of the SP^3 carbon bonds are terminated by C atoms due to the lack of H atoms, leading to the formation of amorphous carbon instead of diamond crystalline.

3.1. Proposed Growth Mechanism of "Cactus" Decorated Nanotubes

3.1.1. Bottom Up Root Growth and Top Down Strong Plasma Induced Carbon Covalent Absorption

During the growth process of CNT, the first requirement is the active catalyst. Generally, a thin layer of iron oxides will be formed on the catalyst surface. Although no NH_3 or H_2 gas is introduced in the growth, C_2H_2 could still be partially decomposed into carbon and hydrogen ions under plasma irradiation at high temperature (700 °C). Previous studies showed that the absorption process of C_2H_2 molecules on the catalyst surface would produce C−H, C and H components.[9] The active H ions produced could reduce the iron oxides to form effective iron catalysts for the nanotube growth. The growth of carbon nanotubes in our work is believed to follow the bottom to up root-growth model.[17, 18] The question is whether the "cactus" appears at the beginning stage or the final stage of the growth process.

In order to resolve this issue, an as-grown normal MWNT sample [SEM image is shown in Fig. 5(a)] was placed into the PECVD chamber for regrowth according to the growth condition of "cactus" nanotube for 1 h. Similar top-decorated "cactus" morphology is obtained, as shown in Figure 5(b). This indicates that the "cactus" does not form bottom-up at the beginning stage. Instead, a top-down strong-plasma induced carbon covalent adsorption mechanism is proposed. Firstly, carbon nanotubes grow following the root growth model. Because of the absence of pretreatment, the decomposition rate of C_2H_2 molecules on the catalytic particle surface is slower, resulting in a higher C_2H_2 concentration in the chamber. Since the plasma can dissociate the hydrocarbon and create a lot of reactive radicals,[8] the enhanced ion bombardment could destroy the outer graphite layers and producing a lot of dangling bonds and amorphous structures, as shown in Figure 3(c) and 3(d). Moreover, the size effect makes the tip more

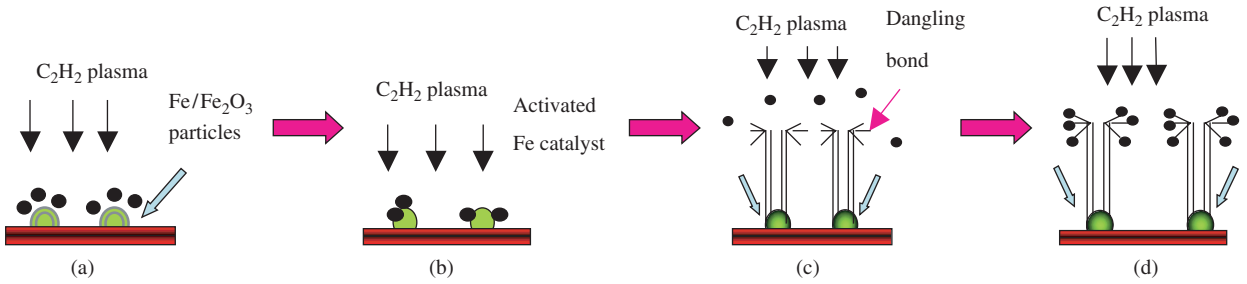

Fig. 6. (a) C_2H_2 is dissociated under the plasma effect at high temperature (b) Iron oxide layer on the iron particles surface is reduced by the dissociated H atoms (c) nanotubes grow following the root growth model, and the dangling bonds are produced under the strong plasma (d) covalent absorption of carbon atoms on the top part.

reactive and enhances atomic absorption, deposition, and reconstruction, thus favoring the formation of the amorphous "cactus". At the same time, the carbon nanotubes continue to grow from bottom to up, since the top "cactus" morphology shields most of the ion bombardment from the lower part. Correspondingly, the covalent absorption of carbon atoms would decrease from top to bottom, producing the different diameters observed in the different parts of the nanotubes. The proposed growth process is illustrated in the detailed schematic as shown in Figure 6. In the case of as-grown MWNT sample, it was also observed that the length of nanotubes is reduced after the regrowth process [shown in Fig. 5(b)]. This can be explained by the termination of the catalytic activity during the regrowth process and the strong ion bombardment effect.

3.2. Third-Order Nonlinear Optical Properties of "Cactus" Nanotubes

To evaluate the third order nonlinearities as well as the relaxation dynamic of this "cactus" top decorated carbon nanotubes grown on quartz substrate, open aperture, closed aperture Z scan as well as the degenerate pump probe experiments were performed at 780 nm. The sample with 2 μm in thickness is prepared for this optical nonlinearities measurement. Figure 7 displays the Z Scan signals. It can be seen from Figure 7 (a) that the nonlinear absorption appears as photo-bleaching signal (increased transmittance with increasing laser intensity) while the refractive index is negative in sign. The photo-bleaching is observed in many SWCNTs,[19, 20] and is believed to due to the state filling effect.[19] It is also observed for MWCNTs.[21, 22] To quantify the observed nonlinear signals, we assume that the nonlinear absorption can be expressed as $\Delta\alpha = \beta I$, and $\Delta n = n_2 I$, where β is the third-order nonlinear absorption coefficient, n_2 the Kerr-type refractive nonlinearity, and I the laser irradiance. Following a Z-scan analytical procedure similar to the one reported in Ref. [21] to fit the experimental curves, we obtain the β and n_2-values to be -20 cmGW^{-1} and -3.2×10^{-4} cm^{2}GW^{-1}, respectively. These two parameters give the value of third-order nonlinear susceptibility $|\chi^{(3)}|$ of 2.2×10^{-11} esu, which is very close to our previous measured result for MWCNTs film,[21] despite the different growth condition and outlook of the two batches of samples. Further Z Scan measurements with different irradiance from 23 GWcm^{-2} to 80 GWcm^{-2} [Fig. 7(b)] show that both β and n_2 are independent on the laser intensity, indicating the pure third order nonlinearity origin to our Z Scan observations.

For pump probe measurement, the intensity of the pump is varied from 5.4 GWcm^{-2} to 24 GWcm^{-2} while the intensity of the probe beam remains at 0.15 GWCm^{-2}.

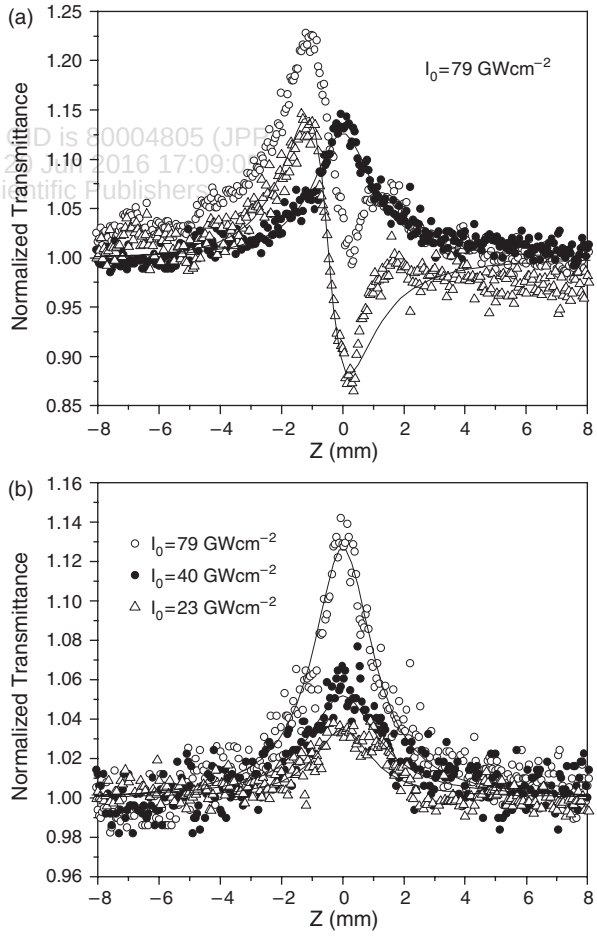

Fig. 7. (a) At $I_0 = 79$ GWcm^{-2}, open aperture (filled circles), close aperture (open circles) Z Scan results. The open triangles are obtained from close aperture curve divided by open aperture curve. The lines are fitting results. (b) Open aperture Z Scan curves at different laser intensity.

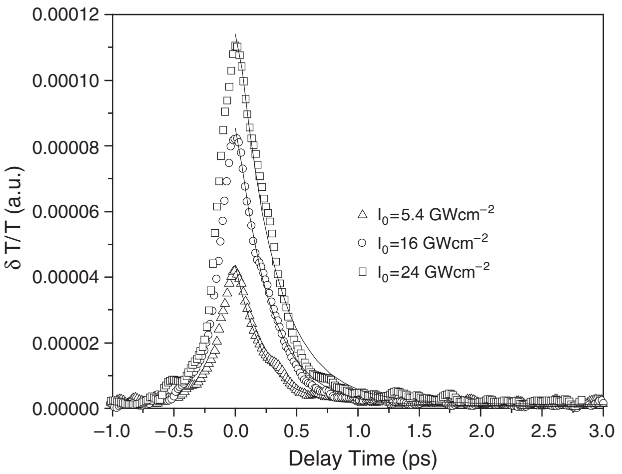

Fig. 8. Degenerate pump probe signal of “cactus” nanotube at 780 nm.

Figure 8 shows the relaxation process of this sample. Two processes can be identified. Fitting the curves with two exponential components, we obtain relaxation time of 260 fs for the faster process and relaxation time of 1 ps for the slower process. The faster decay process is believed to be the autocorrelation of the laser pulses while the slower decay process is associated with the electron–phonon interaction as proposed in Ref. [23]. Figure 8 also shows that though the probe signal increase with the increase of laser beam, the relaxation time remains the same.

To check the effects of the substrate to the measurement results, the substrate was also examined with Z Scan and pump probe experiments. There is no observed photo-bleaching signal up to the laser intensity of 80 GWcm^{-2}, which indicates that the obtained open aperture and pump probe signals are solely from the “cactus” top decorated nanotube film. The closed aperture Z Scan shows that the substrate has a third-order nonlinear refractive index of positive sign, but its magnitude is less than 10% of the n_2 value for the substrate-MWCNT composites so that it can be neglected.

4. CONCLUSIONS

A new morphology of “cactus” top-decorated aligned carbon nanotubes is reported. HRSEM shows that the top “cactus” is composed of a large quantity of nano-sheets. Raman studies reveal a strong defect component in the “cactus” nanotubes compared with that of C_2H_2/NH_3 grown MWNTs. TEM images show the amorphous carbon nature of the top “cactus” morphology. XPS data reveals a higher SP^3 component, which could be attributed to the bonds between SP^3C and C atoms. The possible growth mechanism is also investigated. The activity of catalyst is turned on by the dissociation of C_2H_2 on the nanoparticle surface; while the formation of “cactus” morphology is attributed to plasma induced carbon covalent absorption. The third order nonlinearities are determined with femtosecond Z scan and pump probe techniques at 780 nm. The nonlinear absorption is found to be photo-bleaching type, and the nonlinear absorption coefficient is −20 cmGW^{-1} up to the intensity of 80 GWcm^{-2}. The third-order nonlinear refractive index is -3.2×10^{-4} cm^{2}GW^{-1}. The nonlinear dynamics shows the relaxation process takes place in about 1 ps, which is a characteristic relaxation time for MWCNTs.

References and Notes

1. M. S. Dresselhaus, G. Dresselhaus, and A. Jorio. *Annu. Rev. Mater. Res.* 34, 247 (**2004**).
2. H. Dai, *Surf. Sci.* 500, 218 (**2002**).
3. M. S. Dresselhaus, G. Dresselhaus, J. C. Charlier, and E. Hernandez, *Phil. Trans. R. Soc. Lond. A* 362, 2065 (**2004**).
4. V. Bajpai, L. Dai, and T. Ohashi, *J. Am. Chem. Soc.* 126, 5070 (**2004**).
5. C. J. Lee and J. Park, *Appl. Phys. Lett.* 77, 3397 (**2000**).
6. S. Trasobares, C. P. Ewels, J. Birrell, O. Stephan, B. Q. Wei, J. A. Carlisle, D. Miller, P. Keblinski, and P. M. Ajayan, *Adv. Mater.* 16, 610 (**2004**).
7. Z. F. Ren, Z. P. Huang, J. W. Xu, J. H. Wang, P. Bush, M. P. Siegal, and P. N. Provencio, *Science* 282, 1105 (**1998**).
8. M. Meyyappan, L. Delzeit, A. Cassell, and D. Hash, *Plasma Sources Sci. Technol.* 12, 205 (**2003**).
9. V. Kayastha, Y. K. Yap, S. Dimovski, and Y. Gogotsi, *Appl. Phys. Lett.* 85, 3265 (**2004**).
10. X. J. Yu, O. Wilhelmi, H. O. Moser, S. V. Vidyarai, X. Y. Gao, A. T. S. Wee, T. Nyunt, H. J. Qian, and H. W. Zheng, *J. Electr. Spec. Related Phenomena* 144, 1031 (**2005**).
11. L. Nilsson, O. Groening, C. Emmenegger, O. Kuettel, E. Schaller, and L. Schlapbach, H. Kind, J.-M. Bonard, and K. Kern, *Appl. Phys. Lett.* 76, 2071 (**2000**).
12. N. Chakrapani, S. Curran, B. Wei, and P. M. Ajayan, *J. Mater. Res.* 18, 2515 (**2003**).
13. J. Filik, P. W. May, S. R. J. Pearce, R. K. Wild, and K. R. Hallam, *Diamond Relat. Mater.* 12, 974 (**2003**).
14. H. Ago, T. Kugler, F. Cacialli, W. R. Salaneck, M. S. P. Shaffer, A. H. Windle, and R. H. Friend, *J. Phys. Chem. B* 103, 8116 (**1999**).
15. T. Y. Leung, W. F. Man, P. K. Lim, W. C. Chan, F. Gaspari, and S. Zukotynski, *J. Non-cryst. Solids* 254, 156 (**1999**).
16. L. Sun, J. Gong, D. Zhu, Z. Zhu, and S. He, *Adv. Mater.* 16, 1849 (**2004**).
17. K. Y. Lim, C. H. Sow, J. Lin, F. C. Cheong, Z. X. Shen, J. T. L. Thong, K. C. Chin, and A. T. S. Wee, *Adv. Mater.* 15, 300 (**2003**).
18. S. Fan, M. Chapline, N. Franklin, T. Tombler, A. Cassell, and H. Dai, *Science* 283, 512 (**1999**).
19. J. S. Lauret, C. Voisin, G. Cassabois, C. Delalande, P. H. Roussignol, O. Jost, and L. Capes, *Phys. Rev. Lett.* 90, 057404 (**2003**).
20. Y. C. Chen, N. R. Raravikar, L. S. Schadler, P. M. Ajayan, Y. P. Zhao, T. M. Lu, G. C. Wang, and X. C. Zhang, *Appl. Phys. Lett.* 81, 975 (**2002**).
21. H. I. Elim, W. Ji, G. H. Ma, K. Y. Lim, C. H. Sow, and C. H. A. Huan, *Appl. Phys. Lett.* 85, 1799 (**2004**).
22. Z. Wang, C. Liu, H. Xiang, Z. Li, Q. Gong, Y. Qin, Z. Guo, and D. Zhu, *J. Phys. D: Appl. Phys.* 37, 1079 (**2004**).
23. T. Hertel, R. Fasel, and G. Moos, *Appl. Phys. A* 75, 449 (**2002**).

Received: 29 September 2005. Revised/Accepted: 16 January 2006.